

# $B_\Lambda(^5_\Lambda \text{He})$ from short range effective field theory

L. Contessi<sup>1,a)</sup>, N. Barnea<sup>1</sup> and A. Gal<sup>1</sup>

<sup>1</sup>*Racah Institute of Physics, The Hebrew University, Jerusalem 91904, Israel*

<sup>a)</sup>Corresponding author: contessi.lorenzo@mail.huji.ac.il

**Abstract.** We present an effective field theory (EFT) at leading order to describe light single- $\Lambda$  hypernuclei. Owing to the weak  $\Lambda$  binding and to the  $\Lambda N$  short interaction range, meson exchange forces are approximated by contact interactions within a pionless EFT ( $\#$ EFT) where the only degrees of freedom are baryons. At leading order, the  $\Lambda$ -nuclear interaction contains two 2-body (singlet and triplet) and three 3-body interaction terms, a total of 5 terms associated with 5 coupling strengths or low energy constants (LECs). We adopt the 2-body LECs from hyperon-nucleon scattering data and interaction models that constrain the  $\Lambda N$  scattering lengths, while the 3-body LECs are adjusted using both 3-body and 4-body hypernuclear binding energies. To calculate the binding energies for  $A$ -body systems with  $A > 2$ , we expand the wavefunctions using a correlated Gaussian basis. The stochastic variational method is employed to select the non-linear parameters. The resulting  $\#$ EFT is then applied to calculate the  $\Lambda$  separation energy in  ${}^5_\Lambda \text{He}$ , where the adjusted 3-body interactions largely resolve the known overbinding problem of  ${}^5_\Lambda \text{He}$ .

## INTRODUCTION

The inclusion of a  $\Lambda$  particle in nuclei is the first natural step in extending the periodic table into the strangeness sector. While other hyperons such as  $\Sigma$  and  $\Xi$  might be considered in a theoretical framework, the available hypernuclear data consist almost exclusively of single- $\Lambda$  hypernuclei which present some fascinating questions, and complications, for theory to resolve. In the present work, we aim to address two of several unsolved problems in  $\Lambda$  hypernuclei: (i) the difficulties in establishing precise  $\Lambda N$  scattering parameters from experimental results, and (ii) the so called *overbinding problem* of  ${}^5_\Lambda \text{He}$  in modern  $\Lambda$ -nuclear interactions.

**TABLE 1.** Input scattering lengths (in fm) used to adjust  $\#$ EFT LECs. Except for the Nijmegen models (based on model NSC97f [2]) the listed  $\Lambda N$  scattering lengths are identified with tabulated  $\Lambda p$  scattering lengths.

$\Lambda N$ Fit/Model	Ref.	$a_s(NN)$	$a_s(\Lambda N)$	$a_t(\Lambda N)$	$\bar{a}_{\Lambda N}$
Alexander[A]	[1]	-23.72	-1.8	-1.6	-1.65
Alexander[B]	[1]	-18.63	-1.8	-1.6	-1.65
Nijmegen[A]	[2]	-23.72	-2.60	-1.71	-1.93
Nijmegen[B]	[2]	-18.63	-2.60	-1.71	-1.93
$\chi$ EFT(LO)	[3]	-18.63	-1.91	-1.23	-1.40
$\chi$ EFT(NLO)	[4]	-18.63	-2.91	-1.54	-1.88

The experimental difficulties in measuring  $\Lambda N$  scattering parameters stem from the unavailability of hyperon beams or hyperon targets, thereby limiting all measurements to the use of secondary interactions. Most of the data available in this 2-body sector, which is of great importance for theory, consist of spin-independent  $\Lambda p$  scattering total cross sections at insufficiently low energies [1, 5]. Table 1 demonstrates the uncertainty exhibited by adopting  $\Lambda N$  scattering lengths directly from fits to  $\Lambda p$  scattering cross sections [1] or from several leading hyperon-nucleon (YN) interaction models, with spin-singlet  $a_s(\Lambda N)$  values varying between  $-1.91$  and  $-2.91$  fm and spin-triplet  $a_t(\Lambda N)$  values varying between  $-1.23$  and  $-1.71$  fm. Interestingly, the uncertainty in the listed values of the spin-independent scattering length combination  $\bar{a}_{\Lambda N} = (3/4)a_t + (1/4)a_s$  is somewhat smaller. Hypernuclear data too are not as abundant as nuclear data are. The known  $\Lambda$  hypernuclear binding energies are limited to a few dozens of systems, for many

of which the deduced information is further limited to ground states. In spite of several recent experiments on light hypernuclei [6, 7, 8] our knowledge in this sector remains incomplete. Altogether one is far from having the precision and extension of experimental data that is found in standard nuclear physics.

**TABLE 2.** Ground-state  $\Lambda$  separation energies  $B_\Lambda$  and excitation energies  $E_x$  (in MeV) from several few-body calculations of  $s$ -shell  $\Lambda$  hypernuclei, see text. Charge symmetry breaking is included in the  ${}^4\text{H}$  results from Ref. [15, 16].

Exp.	$B_\Lambda({}^3\text{H})$ 0.13(5) [9]	$B_\Lambda({}^4\text{H}_{\text{g.s.}})$ 2.16(8) [6, 7]	$E_x({}^4\text{H}_{\text{exc.}})$ 1.09(2) [8]	$B_\Lambda({}^5\text{He})$ 3.12(2) [9]
Dalitz et al. [10]	0.10	2.24	0.36	$\geq 5.16$
AFDMC (I)	–	1.97(11) [11]	–	5.1(1) [12]
AFDMC (II)	–1.22(15) [11]	1.07(8) [11]	–	3.22(14) [11]
AFDMC (III)	0.23(9) [13]	1.95(9) [13]	–	2.75(5) [13]
$\chi$ EFT(LO <sub>600</sub> )	0.11(1) [14]	2.31(3) [15, 16]	0.95(15) [15, 16]	5.82(2) [17]
$\chi$ EFT(LO <sub>700</sub> )	–	2.13(3) [15, 16]	1.39(15) [15, 16]	4.43(2) [17]

It is not surprising, given this background, that many interaction models have been formulated to describe hypernuclei. Most of these models describe well the few-body ( $A \leq 4$ ) sector but overbind heavier hypernuclei starting from  ${}^5\text{He}$  which is overbound by 1-2 MeV and for which precise ab initio calculations are still possible. In Table 2 several of the most commonly used interaction models are listed together with their resulting ground-state  $\Lambda$  separation energies  $B_\Lambda$  and excitation energies  $E_x$  for the relevant 3-, 4-, and 5-body hypernuclei. Already in 1972 Dalitz et al. [10] realized that  ${}^5\text{He}$  was overbound by using a phenomenological  $\Lambda N + \Lambda NN$  model, and this overbinding problem has persisted in modern  $\chi$ EFT interaction models [15, 16, 17] at leading order (LO) and for a wide range of cut-off values (calculations for NLO in  $\chi$ EFT have not been reported yet). The only published calculation which seems not to be plagued by the overbinding problem is the one using the AFDMC (II) interaction model [11] which is based on a Bodmer-type  $\Lambda N$  interaction [18] and on refitted Urbana-like  $\Lambda NN$  interactions. However, this interaction model underbinds the 3- and 4-body systems, thus shifting the  ${}^5\text{He}$  overbinding problem to an underbinding problem for the lighter hypernuclei. Recently these authors presented a version of the same interaction, AFDMC (III) [13], in which the  $\Lambda$  separation energies in the 3- and 4-body systems are well reproduced and  ${}^5\text{He}$  is even underbound, implying that  ${}^5\text{He}$  still requires to be fully understood. These calculations suggest that a 2-body  $\Lambda N$  interaction is indeed insufficient to reproduce hypernuclear ground-state separation energies, but also that the mere introduction of 3-body  $\Lambda NN$  interactions does not guarantee that  $B_\Lambda({}^5\text{He})$  is reproduced.

The aim of this report is to show how pionless EFT may be used within error-controlled ab initio few-body calculations to come close to a good reproduction of  $B_\Lambda({}^5\text{He})$  without incurring substantial overbinding. To this end we review and expand on our recent application of  $\chi$ EFT to single  $\Lambda$  hypernuclei [19]. In the following,  $B_\Lambda({}^5\text{He})$  is calculated for all of the input two-body scattering parameters shown in Table 1, thereby linking binding energy calculations of  $s$ -shell hypernuclei directly with  $\Lambda N$  scattering data and  $\Lambda N$  model predictions.

## PIONLESS EFT

Effective field theories rely on the relevant symmetries of the underlying interactions for the phenomena of interest: Quantum Chromo Dynamics for nuclear and hypernuclear physics. In the present problem, the applicable degrees of freedom are baryons, which along with the low values of the exchanged momentum  $Q$  involved justifies the use of a non-relativistic approach. Moreover, since in light ( $A \leq 5$ ) nuclear and hypernuclear systems  $Q$  is small, explicit meson exchange plays an insignificant role while contact (or pionless) potentials become more appropriate. This is especially true for  $\Lambda$  hyperons which are weakly bound in light hypernuclei, but also for standard nuclei with  $A \leq 4$  where the contact approach proved to give exceptionally good results despite the less clear separation of scales [20]. Here we use a regular  $\chi$ EFT approach for the nuclear interaction as described by van Kolck in [21] with two 2-body and one 3-body free parameter and, further, develop a  $\chi$ EFT approach for hypernuclear systems by adding two 2-body  $\Lambda N$  and three 3-body  $\Lambda NN$  interaction terms.

In both cases, nuclei and hypernuclei,  $\chi$ EFT is applied within the same procedure: the interaction at LO assigns one 2-body or a 3-body contact term for each possible 2- and 3-body  $s$ -wave ( $L=0$ ) state. The  $NNN$  and  $\Lambda NN$  contact terms may be viewed as arising dominantly from  $NN \leftrightarrow \Delta N$  and  $\Lambda N \leftrightarrow \Sigma N$  coupled channel interactions,

respectively, promoted from subleading order to LO. Momentum dependent operators, spin-orbit and tensor force, which also appear at subleading order in this approach, are not included in the calculation, as well as the Coulomb interaction. The free parameters of the theory are the LECs which are directly related to the structure of the possible few-body states, and are included in the theory as strengths of zero-range contact interactions. However, because a zero-range interaction is too singular to be used without introducing a regularization/renormalization scheme, it is customary to introduce a Gaussian regulator specified by its momentum cut-off  $\lambda$  (see e.g. [22]):

$$\delta_\lambda(\vec{r}) = \left( \frac{\lambda}{2\sqrt{\pi}} \right)^3 \exp\left(-\frac{\lambda^2}{4}\vec{r}^2\right), \quad (1)$$

thereby making the LECs cut-off dependent. Choosing other local or nonlocal regulators affects mostly the fitted LECs. The resulting LO two-baryon interaction reads then:

$$V_{2B} = \sum_{IS} C_\lambda^{IS} \sum_{i < j} \mathcal{P}_{IS}(ij) \delta_\lambda(\vec{r}_{ij}), \quad (2)$$

where  $\mathcal{P}_{IS}$  are projection operators on  $NN$ ,  $\Lambda N$  pairs with isospin  $I$  and spin  $S$  and the coefficients  $C_\lambda^{IS}$  are the respective LECs. The LO three-body interaction consists of a single  $NNN$  term associated with the  $IS = \frac{1}{2}\frac{1}{2}$  channel, and three  $\Lambda NN$  terms associated with the  $IS = 0\frac{1}{2}, 1\frac{1}{2}, 0\frac{3}{2}$  s-wave configurations, with explicit forms given by

$$V_{NNN} = D_\lambda^{\frac{1}{2}\frac{1}{2}} \sum_{i < j < k} Q_{\frac{1}{2}\frac{1}{2}}(ijk) \left( \sum_{\text{cyc.}} \delta_\lambda(\vec{r}_{ik}) \delta_\lambda(\vec{r}_{jk}) \right), \quad (3)$$

$$V_{\Lambda NN} = \sum_{IS} D_\lambda^{IS} \sum_{i < j} Q_{IS}(ij\Lambda) \delta_\lambda(\vec{r}_{i\Lambda}) \delta_\lambda(\vec{r}_{j\Lambda}), \quad (4)$$

where the first sum in Eq. (3) runs over all  $NNN$  triplets, the second sum in Eq. (4) runs over all  $NN$  pairs,  $Q_{IS}$  are projection operators on baryon triplets with isospin  $I$  and spin  $S$ , and  $D_\lambda^{IS}$  denote the corresponding LECs.

The two nuclear 2-body LECs were fitted here to the deuteron binding energy (2.22 MeV) and two different spin-singlet  $pn$  scattering lengths in the cases Alexander[A] - Alexander[B] and Nijmegen[A] - Nijmegen[B], introduced to test the resilience of the hypernuclear theory against small changes in the nuclear input.  $\Lambda N$  parameters are fitted to the 2-body scattering lengths shown in Table 1. All the other parameterizations have different  $\Lambda N$  scattering lengths as listed in Table 1. Two of the 3-body coefficients were fitted to reproduce  $B(^3\text{H})$  and  $B(^3\Lambda\text{H})$ , but to determine the two remaining  $\Lambda NN$  LECs it is not possible to use any other 3-body system because of the lack of experimental data. Therefore,  $B_\Lambda(^4\text{H}_{\text{g.s.}})$  and  $B_\Lambda(^4\text{H}_{\text{exc.}})$  for the two known levels of the  $A = 4$  isodoublet hypernuclei with spins  $S = 0, 1$ , respectively, have been used.  $B(^4\text{He})$  and  $B_\Lambda(^5\text{He})$  emerge then as predictions of the theory.

In hypernuclei, a one-pion exchange in the  $\Lambda N$  interaction is forbidden by isospin conservation, making two-pion exchange the longest range meson exchange possible and thereby defining an energy breaking scale of  $2m_\pi$ , higher than the scale  $m_\pi$  in the nuclear case. Therefore, we expect a truncation error of order  $(Q/2m_\pi)^2 \sim 9\%$  for the theoretical prediction of  $\Lambda$  separation energies in single  $\Lambda$  hypernuclei, where the momentum scale  $Q$  is provided in light  $\Lambda$  hypernuclei by  $Q \sim p_\Lambda \approx \sqrt{2M_\Lambda B_\Lambda^{\text{exp.}}(^5\text{He})} = 83 \text{ MeV/c.}$

## RESULTS

In the present work, as in [19],  $\pi$ EFT was developed and applied to  $s$ -shell hypernuclei up to  $A \leq 5$  using the Numerov algorithm and the stochastic variational method (SVM) [23] for a range of cut-offs between 1 to 10  $\text{fm}^{-1}$ . The deuteron binding energy  $B_d$ , the 2-body scattering lengths listed in Table 1,  $B(^3\text{H})$ ,  $B(^3\Lambda\text{H})$ ,  $B(^4\text{H}_{\text{g.s.}})$  and  $B(^4\text{H}_{\text{exc.}})$  were used to determine the three nuclear LECs and the five hypernuclear LECs. The  $\Lambda$  separation energy in  ${}^5\Lambda\text{He}$  was evaluated by subtracting  $B(^4\text{He})$  from  $B(^5\Lambda\text{He})$  for all the cut-offs  $\lambda$  considered here. These binding energies were found to depend only moderately on  $\lambda$ , for  $\lambda \gtrsim 2 \text{ fm}^{-1}$ , exhibiting renormalization scale invariance in the limit  $\lambda \rightarrow \infty$ . For example, using  $a_S(NN) = -18.63 \text{ fm}$ , one obtains in this limit  $B(^4\text{He}) \rightarrow 29.2 \pm 0.5 \text{ MeV}$  which compares well with  $B_{\text{exp.}}(^4\text{He}) = 28.3 \text{ MeV}$ , given that our  $\pi$ EFT is truncated at LO and that the Coulomb force should reduce  $B(^4\text{He})$  further by about 1 MeV. Results for  $B_\Lambda(^5\text{He})$  are shown in Figure 1.

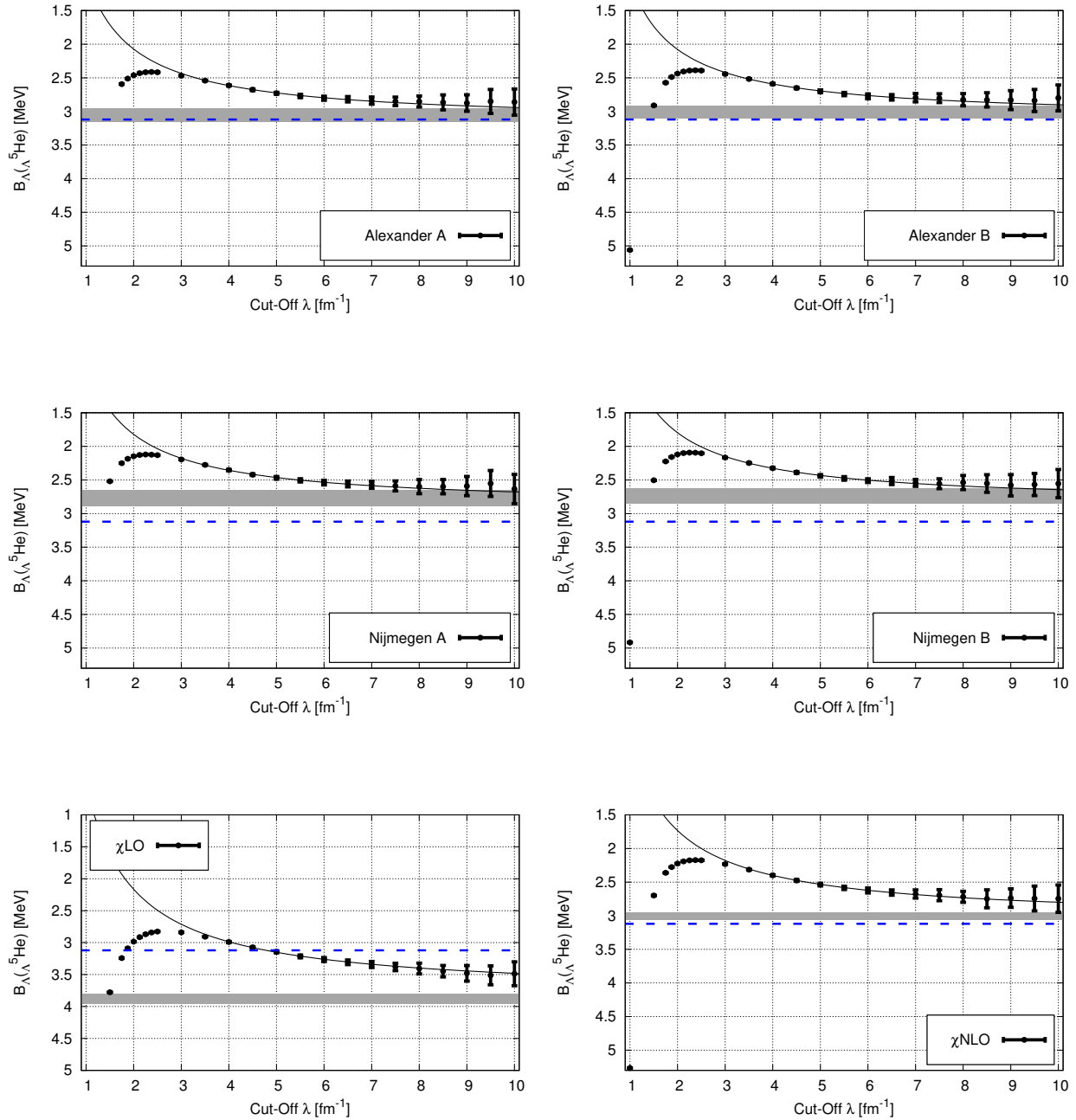


**FIGURE 1.** Dependence of  $B_{\Lambda}(\Lambda^5\text{He})$ , evaluated by subtracting  $B(\Lambda^4\text{He})$  from  $B(\Lambda^5\text{He})$  in SVM calculations, on the  $\chi$ EFT cut-off parameter  $\lambda$ . The black error bars are estimated as the quadratic sum of the numerical errors of the two calculations. The blue dashed lines represent  $B_{\Lambda}^{\text{exp}}(\Lambda^5\text{He})$ , and the gray bands represent the two-parameter extrapolation  $B_{\Lambda}^{\lambda} = B_{\Lambda}^{(\infty)} + a/\lambda$  for  $\lambda \rightarrow \infty$ , fitted starting from  $\lambda=4 \text{ fm}^{-1}$ . These bands include the numerical and extrapolation errors while the truncation error of the theory at LO, estimated as  $\sim 300 \text{ keV}$ , is not included. The data show modest cut-off dependence and RG invariance for  $\lambda \geq 3 \text{ fm}^{-1}$ . The extrapolated  $B_{\Lambda}(\Lambda^5\text{He})$  values using the Alexander or the  $\chi$ EFT(NLO) parameterizations are in good agreement with  $B_{\Lambda}^{\text{exp}}(\Lambda^5\text{He})$ , whereas  $\chi$ EFT(LO) reproduces it better than the other models do for finite cut-off values  $\lambda \sim 2-4 \text{ fm}^{-1}$ . The upper first and second groups of graphs represent the results of using the Alexander and the Nijmegen  $\Lambda N$  scattering model inputs, respectively, each one with two assumed values  $a_s(NN)=-18.63$  and  $-23.72 \text{ fm}$ , hardly affecting the extrapolation  $B_{\Lambda}(\Lambda^5\text{He})$  value.

The calculated  $\Lambda$  separation energies were extrapolated to infinite cut-off  $\lambda \rightarrow \infty$  using inverse power expansion as suggested by  $\#$ EFT:  $B_{\Lambda}^{\lambda} = B_{\Lambda}^{(\infty)} + a/\lambda + O(1/\lambda^2)$ . In Figure 1, the extrapolated values  $B_{\Lambda}^{(\infty)}$  are represented by gray bands which account for the calculational uncertainty and the estimated systematic extrapolation error. Truncation errors, due to not including subleading orders in the theory, are listed in Table 3.

**TABLE 3.**  $B_{\Lambda}(\Lambda^5\text{He})$  values (MeV) in LO  $\#$ EFT calculations, with cut-off parameters  $\lambda=4 \text{ fm}^{-1}$  and  $\lambda \rightarrow \infty$  (see text) for several choices of  $\Lambda N$  interaction model. The uncertainties for  $\lambda=4 \text{ fm}^{-1}$  are due to subtracting  $B(^4\text{He})$  from  $B(\Lambda^5\text{He})$ , whereas those for  $\lambda \rightarrow \infty$  represent (i) the numerical error and systematic uncertainty from the extrapolation, and (ii) the LO truncation error, respectively.

$B_{\Lambda}(\Lambda^5\text{He})$	Alexander[A]	Alexander[B]	Nijmegen[A]	Nijmegen[B]	$\chi$ LO	$\chi$ NLO
$\lambda=4 \text{ fm}^{-1}$	2.61(3)	2.59(3)	2.35(3)	2.32(3)	2.99(3)	2.40(3)
$\lambda \rightarrow \infty$	3.06(10)(30)	3.01(10)(30)	2.77(12)(30)	2.74(11)(30)	3.96(08)(35)	3.01(06)(30)

The  $B_{\Lambda}(\Lambda^5\text{He})$  values shown in Fig. 1 vary from a moderate underbinding for  $\lambda \geq 1.5 \text{ fm}^{-1}$ , with a maximum around  $\lambda=2-3 \text{ fm}^{-1}$ , to few MeV of overbinding for smaller cut-offs, comparable with overbindings produced in other interaction models described in the Introduction. The graphs highlight a convergent pattern between  $\lambda=4$  and  $10 \text{ fm}^{-1}$ , with a moderate cut-off dependence when  $\lambda > 2 \text{ fm}^{-1}$ . The extrapolated result is in good agreement with the experimental value of  $B_{\Lambda}(\Lambda^5\text{He})$  upon using the experimentally-based Alexander ([A] or [B]) parametrization and also the  $\chi$ EFT(NLO) parametrization. The parametrization of  $a_{\Lambda N}$  extracted from  $\chi$ EFT(LO) leads to overbinding of  $\sim 1 \text{ MeV}$ , while  $a_{\Lambda N}$  based on the soft-core Nijmegen model ([A] or [B]) leads even to underbinding of a few hundreds of keV. We conclude that  $\#$ EFT applications at LO prefer the smaller input values of  $a_t(\Lambda N)$  from Table 1. The extrapolations also show that changing slightly the nuclear input (from Alexander[A] to Alexander[B] or from Nijmegen[A] to Nijmegen[B]) hardly affects the final results, suggesting that the hypernuclear applications are only weakly affected by the nuclear interaction input used.

### Relevant cut-offs

The results shown in Fig. 1 and Table 3 allow different interpretations than the one arrived at by extrapolating to  $\lambda \rightarrow \infty$ . While a normal  $\#$ EFT prescription is to extrapolate the results to large values of  $\lambda$  in order to drop residual cut-off dependence, the cut-off may be taken to reproduce a physically reasonable momentum scale between  $\lambda=2$  to  $3 \text{ fm}^{-1}$  which represents a mass scale larger than the  $\#$ EFT breaking scale  $\sim 2m_{\pi}$  but smaller than vector-meson masses starting at  $\approx 4 \text{ fm}^{-1}$ . Here we disregard possible pseudoscalar  $K$ -meson exchange contributions ( $m_K \approx 2.5 \text{ fm}^{-1}$ ) which are known to be insignificant [24]. In this case,  $\chi$ EFT(LO) gives results closer to experiment for  $\Lambda^5\text{He}$  than the other models do.

**TABLE 4.** Effective range values  $r_0$  of  $s$ -wave  $NN$  and  $\Lambda N$  states, and cut-off values  $\lambda_0$  that reproduce these listed values of  $r_0$ .

	$S(NN) = 0$	$S(NN) = 1$	$S(\Lambda N) = 0$	$S(\Lambda N) = 1$
$r_0 \text{ [fm]}$	2.75 [25]	1.74 [25]	3.0 [1]	3.1[1]
$\lambda_0 \text{ [fm}^{-1}]$	1.11	1.30	1.47	1.48

Another possibly relevant cut-off choice is one in which the regulated contact interaction reproduces the effective range  $r_0$  of the two body system. According to the Wigner Bound theorem [26, 27] it is not possible to fix the effective range of the system with contact interactions in LO- $\#$ EFT for  $\lambda \rightarrow \infty$ . In fact,  $\#$ EFT orders are in a one-to-one correspondence with effective-range expansion parameters in two body systems, the LO of the theory is associated with the 2-body scattering length in  $s$ -wave and further parameters can only be described by considering subleading corrections. However, this correspondence holds only in the limit of large cut-offs, and for each finite  $\lambda$  it is possible to associate a finite value of the effective range. In Figure 2a we plot the effective ranges for the four possible 2-body systems described in this work as a function of the cut-off  $\lambda$ ;  $r_0^{(20)}$  and  $r_0^{(\Lambda 0)}$  represent the spin singlet effective range in the nuclear and hypernuclear sectors, respectively, and  $r_0^{(02)}$  and  $r_0^{(\Lambda 2)}$  represent the ones in the spin triplet channel. The experimentally derived values of these effective ranges are listed in Table 4 together with cut-off values  $\lambda_0$  that reproduce these actual effective ranges. Values of  $\sim 3 \text{ fm}$  for the  $\Lambda N$  effective ranges, as listed in Table 1 and marked in Figure 2a, hold in most of the  $\Lambda N$  interaction models listed in Table 1.

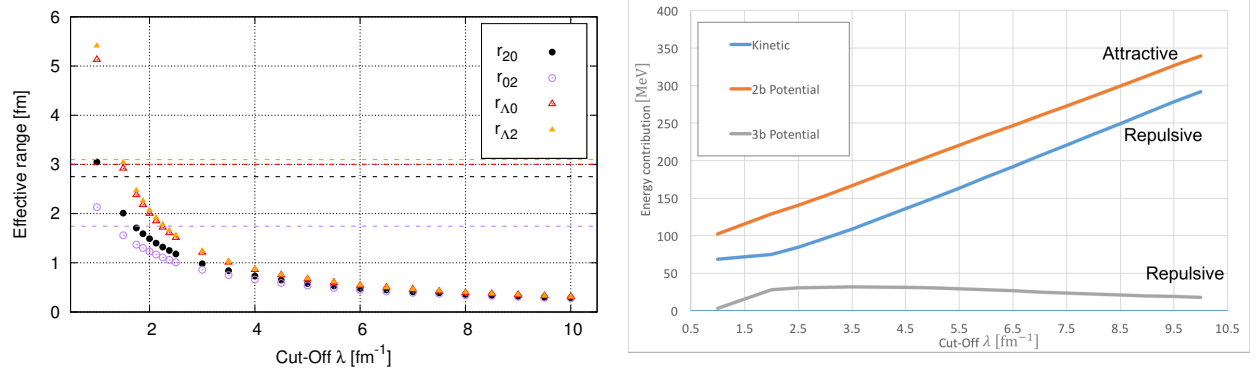


**FIGURE 2.** **a)** Effective range as a function of the cut-off parameter of Gaussian regulators in the four possible two-body  $s$ -wave systems  $NN$  and  $\Lambda N$ , using the choice Alexander[B] for  $a_s(NN)$ . Dashed lines represent experimental values for the  $NN$  effective range parameters ( $r_0^{20}$  in spin singlet,  $r_0^{02}$  in spin triplet) and  $\Lambda N$  effective range parameters suggested by Alexander et al. [1] ( $r_0^{10}$  in spin singlet,  $r_0^{12}$  in spin triplet), all are listed in Table 4. **b)** Potential and kinetic energy expectation values as functions of the cut-off parameter  $\lambda$  in  $^5_{\Lambda}\text{He}$   $\#$ EFT calculations. The kinetic energy and the 3-body potential energy are repulsive for all cut-offs, except for  $\Lambda \sim 1 \text{ fm}^{-1}$  for which the 3-body potential energy gives a small but attractive contribution. The kinetic (repulsive) energy and the 2-body potential (attractive) energy diverge as  $\lambda \rightarrow \infty$ , but their sum remains finite as does the relatively small 3-body potential energy.

It is remarkable that the cut-off values  $\lambda_0$  are close to the ones corresponding to the crossing of the  $B_{\Lambda}({}^5_{\Lambda}\text{He})$  curves as a function of  $\lambda$  with the value  $B_{\Lambda}^{\text{exp.}}({}^5_{\Lambda}\text{He})$  in Figure 1. Indeed, fitting the cut-off to the effective range practically brings in subleading-order contributions that are likely to enhance the predictive precision of the theory. However, this procedure is not guaranteed to have the same outcome for all systems, and the predictability regarding the truncation uncertainty of the theory is partly lost because of powers of  $(Q/\lambda)$  which do not disappear in the expansion parameters of successive orders of the EFT.

Another interesting case of cut-off is  $\lambda \sim 1 \text{ fm}^{-1}$ , where the interaction is relatively of long range, similar to that of one pion exchange. In this case, we recover many features arising in other calculations, such as a slightly attractive 3-body potential along with  ${}^5_{\Lambda}\text{He}$  overbound by as much as 1 – 2 MeV.

### Energy expectation values

The 3-body interaction plays a fundamental role in the  $\#$ EFT description of hypernuclei. On the one hand it prevents by design  $A = 3$  systems from Thomas collapse [28], and on the other hand it fine-tunes the interaction to reproduce the experimental data. The interaction shape becomes stiffer with large cut-off  $\lambda$ s and, as shown in Fig. 2b for  ${}^5_{\Lambda}\text{He}$ , the 2-body potential energy and kinetic energy each diverge, although their sum as well as the 3-body potential energy remain finite. This behavior might appear unexpected, since in the absence of 3-body forces the 2-body potential energy diverges without getting fully compensated by the kinetic energy, thereby leading to collapse. The resolution of this paradox is that the 3-body interaction is extremely stiff and the sizable repulsion induced when three baryons move closer creates a strong correlation between triplets that suppresses the wavefunction, consequently reducing the 3-body potential energy expectation value.

### CONCLUSION

In this report we reviewed and expanded on our recent application of  $\#$ EFT to single  $\Lambda$  hypernuclei [19]. The developed theory extends the standard formulation of  $\#$ EFT at LO for nuclei that uses three nuclear LECs, fitted to nuclear 2- and 3-body observables, by adding five new LECs fitted to hypernuclear 2-, 3- and 4-body observables. The two 2-body  $\Lambda N$  LECs were determined using a wide range of input models and experimental data to account for the large uncertainty involved in extracting reliable values of the  $\Lambda N$  scattering lengths.  $A = 3$  hypernuclear systems other than the observed  ${}^3_{\Lambda}\text{H}$  g.s. with spin 1/2 were not involved in the fitting procedure while also not showing any sign

of being bound or almost bound. In this scheme  $B(^4\text{He})$  and  $B(^5_\Lambda\text{He})$  are a prediction of the theory and are compared with experimental data.

No alarming divergences are found in  $B_\Lambda(^5\text{He})$  and the results for  $\lambda \rightarrow \infty$  differ from the experimental value from an underbinding of few hundred of keV to overbinding of almost 1 MeV, depending on the input 2-body model on which the theory is based. The theory shows good agreement with the experimental data for the extrapolated result both using the experimental parametrization and the scattering parameters extracted from the  $\chi$ EFT(NLO) model. The  $\chi$ EFT(LO) parametrization leads to a slight overbinding in the extrapolated result, but for cut-off values around the breaking scale ( $\lambda \sim 2 - 4 \text{ fm}^{-1}$ ) it reproduces the experimental value more accurately than the other models do.

We have demonstrated how it is possible to develop a  $\chi$ EFT which correlates the solution to the overbinding problem of single  $\Lambda$   $s$ -shell hypernuclei with tested  $\Lambda N$  2-body input parameters. The results suggest a larger dependence of  $B_\Lambda(^5\text{He})$  on the  $\Lambda N$  spin-triplet interaction than on the spin-singlet, implying that fairly small values of triplet scattering lengths (roughly between  $-1.5$  to  $-1.7 \text{ fm}$ ) are favored in order to overcome the overbinding problem.

Lastly, we compared the kinetic energy and the 2- and 3-body potential energy expectation values, noticing a monotonic increase of the 2-body potential energy and the kinetic energy upon increasing the cut-off, while the three-body potential energy reaches a maximum value for cut-off values  $\lambda \sim 5 \text{ fm}^{-1}$ . This behavior is intimately connected to the role played by the  $NNN$  interaction in averting collapse for  $A \geq 3$  and by the  $\Lambda NN$  interaction in fine-tuning the calculated  $\Lambda$  separation energy in  $s$ -shell hypernuclei.

## ACKNOWLEDGMENTS

The work of LC and NB was supported by the Pazy Foundation and by the Israel Science Foundation grant 1308/16.

## REFERENCES

- [1] G. Alexander, U. Karshon, A. Shapira, G. Yekutieli, R. Engelmann, H. Filthuth, and W. Lughofer. Study of the  $\Lambda N$  system in low-energy  $\Lambda p$  elastic scattering. *Phys. Rev.*, 173:1452–1460, 1968.
- [2] Th. A. Rijken, V. G. J. Stoks, and Y. Yamamoto. Soft-core hyperon-nucleon potentials. *Phys. Rev. C*, 59:21–40, 1999.
- [3] H. Polinder, J. Haidenbauer, and Ulf-G. Meißner. Hyperon - nucleon interactions - a chiral effective field theory approach. *Nucl. Phys. A*, 779:244 – 266, 2006.
- [4] J. Haidenbauer, S. Petschauer, N. Kaiser, U.-G. Meißner, A. Nogga, and W. Weise. Hyperon - nucleon interaction at next-to-leading order in chiral effective field theory. *Nucl. Phys. A*, 915:24 – 58, 2013.
- [5] B. Sechi-Zorn, B. Kehoe, J. Twitty, and R. A. Bernstein. Low-energy  $\Lambda$ -proton elastic scattering. *Phys. Rev.*, 175:1735–1740, 1968.
- [6] A. Esser et al. Observation of  ${}^4_\Lambda\text{H}$  hyperhydrogen by decay-pion spectroscopy in electron scattering. *Phys. Rev. Lett.*, 114, 2015.
- [7] F. Schulz et al. Ground-state binding energy of  ${}^4_\Lambda\text{H}$  from high-resolution decay-pion spectroscopy. *Nucl. Phys. A*, 954:149 – 160, 2016.
- [8] T. O. Yamamoto et al. Observation of spin-dependent charge symmetry breaking in  $\Lambda N$  interaction: Gamma-ray spectroscopy of  ${}^4_\Lambda\text{He}$ . *Phys. Rev. Lett.*, 115:222501, 2015.
- [9] D.H. Davis. 50 years of hypernucl. phys.: I. the early experiments. *Nucl. Phys. A*, 754:3 – 13, 2005.
- [10] R.H. Dalitz, R.C. Herndon, and Y.C. Tang. Phenomenological study of  $s$ -shell hypernuclei with  $\Lambda N$  and  $\Lambda NN$  potentials. *Nucl. Phys. B*, 47:109 – 137, 1972.
- [11] D. Lonardoni, F. Pederiva, and S. Gandolfi. Accurate determination of the interaction between  $\Lambda$  hyperons and nucleons from auxiliary field diffusion monte carlo calculations. *Phys. Rev. C*, 89:014314, 2014.
- [12] D. Lonardoni, S. Gandolfi, and F. Pederiva. Effects of the two-body and three-body hyperon-nucleon interactions in  $\Lambda$  hypernuclei. *Phys. Rev. C*, 87:041303, 2013.
- [13] D. Lonardoni and F. Pederiva. Medium-mass hypernuclei and the nucleon-isospin dependence of the three-body hyperon-nucleon-nucleon force. *arXiv:1711.07521v3*, 2018.
- [14] R. Wirth, D. Gazda, P. Navrátil, A. Calci, J. Langhammer, and R. Roth. Ab initio description of  $p$ -shell hypernuclei. *Phys. Rev. Lett.*, 113:192502, 2014.
- [15] D. Gazda and A. Gal. Ab initio calculations of charge symmetry breaking in the  $A=4$  hypernuclei. *Phys. Rev. Lett.*, 116:122501, 2016.

- [16] D. Gazda and A. Gal. Charge symmetry breaking in the  $A=4$  hypernuclei. *Nucl. Phys. A*, 954:161 – 175, 2016.
- [17] R. Wirth and R. Roth. Light neutron-rich hypernuclei from the importance-truncated no-core shell model. *Phys. Lett. B*, 779:336 – 341, 2018.
- [18] A. R. Bodmer, Q. N. Usmani, and J. Carlson. Binding energies of hypernuclei and three-body  $\Lambda$ NN forces. *Phys. Rev. C*, 29:684–687, 1984.
- [19] L. Contessi, N. Barnea, and A. Gal. Resolving the  $\Lambda$  hypernuclear overbinding problem in pionless effective field theory. *Phys. Rev. Lett.*, 121:102502, 2018.
- [20] N. Barnea, L. Contessi, D. Gazit, F. Pederiva, and U. van Kolck. Effective field theory for lattice nuclei. *Phys. Rev. Lett.*, 114:052501, 2015.
- [21] U. van Kolck. Effective field theory of short-range forces. *Nucl. Phys. A*, 645:273 – 302, 1999.
- [22] Betzalel Bazak, Moti Eliyahu, and Ubirajara van Kolck. Effective field theory for few-boson systems. *Phys. Rev. A*, 94:052502, 2016.
- [23] Y. Suzuki and K. Varga. *Stochastic Variational Approach to Quantum-Mechanical Few-Body Problems*. Lecture Notes in Physics Monographs. Springer Berlin Heidelberg, 1998.
- [24] D. J. Millener, A. Gal, C. B. Dover, and R. H. Dalitz. Spin dependence of the  $\Lambda$ n effective interaction. *Phys. Rev. C*, 31:499–509, 1985.
- [25] R. W. Hackenburg. Neutron-proton effective range parameters and zero-energy shape dependence. *Phys. Rev.*, C73:044002, 2006.
- [26] E. P. Wigner. Lower limit for the energy derivative of the scattering phase shift. *Phys. Rev.*, 98:145–147, 1955.
- [27] H. W. Hammer and Dean Lee. Causality and the effective range expansion. *Ann. Phys.*, 325:2212–2233, 2010.
- [28] L. H. Thomas. The interaction between a neutron and a proton and the structure of  $H^3$ . *Phys. Rev.*, 47:903–909, 1935.